INTERNATIONAL JOURNAL FOR NUMERICAL METHODS IN FLUIDS, VOL. 4, 1101–1115 (1984)

EFFICIENT ADI AND SPLINE ADI METHODS FOR THE STEADY-STATE NAVIER-STOKES EQUATIONS

MICHELE NAPOLITANO

Istituto di Macchine, Università di Bari, via Re David 200, 70125 Bari, Italy

SUMMARY

The present paper provides an improved alternating direction implicit (ADI) technique as well as a high-order-accurate spline ADI method for the numerical solution of steady two-dimensional incompressible viscous flow problems. The vorticity–stream function Navier–Stokes equations are considered in a general curvilinear coordinate system, which maps an arbitrary two-dimensional flow domain in the physical plane into a rectangle in the computational plane. The stream function equation is parabolized in time by means of a relaxation-like time derivative and the steady state solution is obtained by a time-marching ADI method requiring to solve only 2×2 block-tridiagonal linear systems. The difference equations are written in incremental form; upwind differences are used for the incremental variables, for stability, whereas central differences approximate the non-incremental terms, for accuracy, so that, at convergence, the solution is free of numerical viscosity and second-order accurate. The high-order-accurate spline ADI technique proceeds in the same manner; in addition, at the end of each two-sweep ADI cycle, the solution is corrected by means of a fifth-order spline interpolating polynomial along each row and column of the computational grid, explicitly. The validity and the efficiency of the present methods are demonstrated by means of three test problems.

KEY WORDS Numerical Solution Navier–Stokes Equations 2-D Steady, Laminar Flows ADI Method Spline Interpolating Polynomials

1. INTRODUCTION

The present author has developed an alternating direction implicit (ADI) technique for the calculation of viscous, incompressible, steady flows past an arbitrary, two-dimensional body.[1] Such an approach used the vorticity–stream function Navier–Stokes equations in a system of general body-fitted coordinates. The governing equations were parabolized by adding a relaxation-like time derivative to the stream function equation, linearized in time and solved by means of the ADI procedure of Douglas and Gunn.[2] The method used second-order-accurate finite differences and, at convergence, provided a second-order-accurate approximation to the steady flow of interest. The major limitation of the proposed ADI approach was due to its use of central differences, which limited its applicability to low Reynolds number flows, or to separation-free high Reynolds number flows. A first-order-accurate method, using upwind differences for the convective terms in the equations, although feasible in principle, is not recommended, insofar as the effective Reynolds number of the numerical solution is lowered by the numerical viscosity introduced by the first-order-accurate upwind differences. A more stable, viscosity-free numerical technique is obtainable by using upwind differences for the convective terms, which are evaluated implicitly, and correcting them to second-order-accurate central differences, explicitly,[3] or, more simply, by employing the incremental (delta) form of the equations[4] and using upwind differences for the incremental variables and central differences for the non-incremental variables. Both

0271–2091/84/12 1101–15$01.50
© 1984 by John Wiley & Sons, Ltd.
Received 6 September 1983
Revised 9 January 1984

approaches, which are shown here to coincide, have the desirable property of lowering the effective Reynolds number of the pseudo-transient problem by adding numerical viscosity, which is, however, completely removed from the solution as convergence is achieved. The second approach, using the incremental variables, is employed in this paper to provide an improved version of the ADI technique given in Reference 1, which is more stable and capable of resolving high Reynolds number separated flows, while maintaining the second-order accuracy of the numerical-viscosity-free central differences, at convergence.

Furthermore, following the idea of Rubin and Khosla,[5] it is possible and very straightforward indeed to obtain a fourth-order-accurate spline ADI method by means of a spline deferred-corrector approach.[5] The present paper also provides a simplified spline ADI technique for the vorticity–stream function Navier–Stokes equations, which has all the features of the aforementioned improved ADI method. In particular, incremental variables are used and, in order to enhance the stability of the method, the convective terms are approximated by first-order-accurate upwind differences. At the end of each two-sweep ADI cycle, the right-hand side (RHS) of the difference equations, which is already second-order accurate, is corrected by means of a spline interpolating procedure, explicitly, so that, at convergence, a fourth-order-accurate approximation to the steady flow of interest is obtained.

The present paper develops as follows: in Section 2 the basic ideas of obtaining second- or fourth-order accuracy at convergence, while using first-order-accurate upwind differences to stabilize the transient phenomenon, are provided. The approach of Rubin and Khosla[3,5] is briefly reviewed and the equivalent simpler and more elegant approach used in this study is presented. In Section 3 those ideas are applied to the ADI numerical technique previously developed by the author,[1] to provide an improved, more stable, second-order-accurate ADI method as well as a fourth-order-accurate spline ADI procedure.

Finally, the results obtained by applying the present techniques to two model problems (viscous flow between two concentric circles and the classical driven cavity flow) as well as to a problem of practical interest (viscous flow in a channel of complex geometry) are presented in Section 4.

2. THE DEFERRED-CORRECTOR APPROACH OF RUBIN AND KHOSLA

Rubin and Khosla have presented their simplified spline technique,[5] as applied to the numerical solution of the steady-state Burgers' equation, starting from the unsteady equation:

$$u_t + cu_x = vu_{xx} \tag{1}$$

The numerical procedure of Rubin and Khosla uses the following discrete form of equation (1), for positive values of the constant, c:

$$\begin{aligned} &u_j^{n+1} - u_j^n + cA(u_j^{n+1} - u_{j-1}^{n+1})k/h - Bv(u_{j+1}^{n+1} - 2u_j^{n+1} + u_{j-1}^{n+1})k/h^2 \\ &\quad = c\{A(u_j^n - u_{j-1}^n) - hm_j^n\}k/h + vk\{M_j^n - B(u_{j+1}^n - 2u_j^n + u_{j-1}^n)/h^2\} \end{aligned} \tag{2}$$

where the subscripts j, $j-1$ and $J+1$ indicate the spatial grid locations, the superscripts n and $n+1$ indicate the old and new time levels, k is the time step, h is the spatial mesh width, m and M are the fourth-order-accurate spline approximations of u_x and u_{xx} and A and B are two arbitrary constants, necessary for the stability of the method; see Reference 5 for details. Notice that the high-order spline correction terms only appear at the old time level, known RHS of equation (2), so that at each time advancement only a tridiagonal system has to be solved (exactly as for the case of a low-order-accurate finite difference scheme), but that, at convergence, a fourth-order-accurate solution is obtained. Also notice that, if m and M are replaced with simple second-order-accurate

finite difference approximations, equation (2) leads to the unconditionally stable KR scheme ($A = B = 1$) of Reference 3.

In the present paper an ADI technique and a spline ADI technique will be developed for the Navier–Stokes equations, which are based on these two techniques. However, an incremental (delta) formulation is preferred in this paper for its superior simplicity and elegance. For example, by writing equation (2) in delta form, one obtains:

$$Du_j + cA(Du_j - Du_{j-1})k/h - Bv(Du_{j+1} - 2Du_j + Du_{j-1})k/h^2 = -ckm_j^n + vkM_j^n \tag{3}$$

where $Du = u^{n+1} - u^n$. Equation (3) actually coincides with equation (2) and will obviously produce the same numerical results, but it is simpler, more elegant and requires less computation effort. Notice, for example, that the RHS of equation (3) is a fourth-order-accurate discrete approximation of the steady Burgers' equation, which thus, at convergence ($Du = 0$ at all grid points), will be resolved with the desired level of accuracy. Moreover, the arbitrary constants A and B, which only multiply the incremental variables, are clearly seen not to influence the final steady-state solution. By comparing the simplicity of equation (3) with respect to equation (2), it is easy to understand the advantage of using the delta approach in complex numerical techniques for the Navier–Stokes equations. Obviously, also in equation (3), by replacing m and M with standard second-order-accurate finite differences, one obtains a scheme which has the stability of a windward difference scheme and the accuracy (at convergence) of a central difference scheme. In such a case, although unnecessary for stability, the use of values greater than one for A and B can further enhance the convergence of the numerical method. It remains to be said how m and M are evaluated. After all $n + 1$ values have been obtained directly from equation (2), or from equation (3) and the definition of Du, the new time level m and M values are explicitly evaluated as

$$m_j = (u_{j+1} - u_{j-1})/2h + h(K_{j-1} - K_{j+1})/12 \tag{4}$$

and

$$M_j = \{K_j + (u_{j+1} - 2u_j + u_{j-1})/h^2\}/2 \tag{5}$$

where all K_j terms are easily obtained by solving the following tridiagonal system:

$$K_{j+1} + 4K_j + K_{j-1} = 6(u_{j+1} - 2u_j + u_{j-1})/h^2 \tag{6}$$

see References 5 or 6 for details. It is noteworthy that, with respect to a standard second-order-accurate finite difference method, the simplified spline technique requires the solution of an additional tridiagonal system (equation (6)), at each time level, whereas a standard spline technique[6] would require the solution of a 2×2 block-tridiagonal system, at each time level. The convenience of the simplified approach is seen to increase when dealing with coupled systems of equations (e.g. with the Navier–Stokes equations).

3. THE PRESENT ADI AND SIMPLIFIED SPLINE ADI METHODS FOR THE NAVIER–STOKES EQUATIONS

The vorticity–stream function Navier–Stokes equations in a general system of curvilinear body-oriented coordinates (ξ, η) are given[7] as:

$$\omega_t + (\psi_\eta \omega_\xi - \psi_\xi \omega_\eta)/J - (\alpha\omega_{\xi\xi} - 2\beta\omega_{\xi\eta} + \gamma\omega_{\eta\eta} + \sigma\omega_\eta + \tau\omega_\xi)/J^2 Re = 0 \tag{7}$$

and

$$(\alpha\psi_{\xi\xi} - 2\beta\psi_{\xi\eta} + \gamma\psi_{\eta\eta} + \sigma\psi_\eta + \tau\psi_\xi)/J^2 + \omega = \psi_t \tag{8}$$

where α, β, γ, σ and τ are the metric coefficients and J is the Jacobian of the coordinate transformation, and a relaxation-like time derivative has been added to the stream function

equation, in order to deal with a parabolic system of equations.[1,8] For this reason, equations (7) and (8) are not the time-dependent Navier–Stokes equations, and in the present time-marching numerical techniques only the converged solutions will have physical meaning.

Equations (7) and (8) are written in terms of the incremental variables, $D\psi = \psi^{n+1} - \psi^n$, $D\omega = \omega^{n+1} - \omega^n$, and linearized in time by a Taylor's series expansion, which neglects terms of order D^2, to give

$$D\omega/k + (D\psi_\eta \omega_\xi^n + \psi_\eta^n D\omega_\xi - D\psi_\xi \omega_\eta^n - \psi_\xi^n D\omega_\eta)/J - (\alpha D\omega_{\xi\xi} + \gamma D\omega_{\eta\eta} + \sigma D\omega_\eta + \tau D\omega_\xi)/J^2 Re = \mathrm{SSVE}^n \tag{9}$$

and

$$D\psi/k - D\omega - (\alpha D\psi_{\xi\xi} + \gamma D\psi_{\eta\eta} + \sigma D\psi_\eta + \tau D\psi_\xi)/J^2 = \mathrm{SSSFE}^n \tag{10}$$

where SSVE^n and SSSFE^n are shorthand notations for steady-state vorticity (stream function) equation evaluated at the n time level. It is noteworthy that the linearized equations (9) and (10) are fully implicit for the incremental variables except for the mixed derivatives, which are treated explicitly. Also, for more generality, two constants, A and B, can be introduced to multiply all convective and diffusive incremental terms, respectively. At this point, we are ready to solve equations (9) and (10) by means of two-sweep ADI techniques, differing only in the level of accuracy used to approximate SSVE^n and SSSFE^n. These ADI methods, derived from that of Douglas and Gunn,[2] proceed as follows: at the first sweep, the η derivatives and the source-like terms in the LHS (left-hand side) of equations (9) and (10) are evaluated implicitly to give:

$$D\tilde{\omega}/k + (D\tilde{\psi}_\eta \omega_\xi - \psi_\xi D\tilde{\omega}_\eta)/J - (\gamma D\tilde{\omega}_{\eta\eta} + \sigma D\tilde{\omega}_\eta)/J^2 Re = \mathrm{SSVE}^n \tag{11}$$

$$D\tilde{\psi}/k - D\tilde{\omega} - (\gamma D\tilde{\psi}_{\eta\eta} + \sigma D\tilde{\psi}_\eta)/J^2 = \mathrm{SSSFE}^n \tag{12}$$

where the $\sim$ indicate that the solution is a first sweep (predictor-type) one and all the ξ derivatives, which are evaluated explicitly, give zero contribution in the incremental variables. At the second and final sweep, all the ξ derivatives and the source-like terms are evaluated implicitly, whereas the η derivatives are evaluated at the first sweep ($\sim$) level, explicitly. The resulting equations are not given here because, for computational convenience, they are replaced by the following ones, obtained by subtracting from them the first sweep equations (11) and (12):

$$D\omega/k + (\psi_\eta^n D\omega_\xi - D\psi_\xi \omega_\eta^n)/J - (\alpha D\omega_{\xi\xi} + \tau D\omega_\xi)/J^2 Re = D\tilde{\omega}/k \tag{13}$$

$$D\psi/k - D\omega - (\alpha D\psi_{\xi\xi} + \tau D\psi_\xi)/J^2 = D\tilde{\psi}/k - D\tilde{\omega} \tag{14}$$

In equations (11)–(14) all the incremental terms are approximated with central differences (the second derivatives) and windward differences (the first derivatives) whereas the non-incremental terms are approximated with standard central differences (for the case of the ADI method) or fourth-order-accurate spline approximations (for the case of the spline ADI method). Therefore, for both techniques, a series of 2×2 block-tridiagonal systems is to be solved at each sweep of the ADI procedure, exactly as in the former ADI technique due to the author.[1]

At the end of a complete ADI cycle the solution is updated as:

$$\psi^{n+1} = \psi^n + D\psi \tag{15}$$

$$\omega^{n+1} = \omega^n + D\omega \tag{16}$$

and, for the case of the ADI method, the process is repeated until a satisfactory convergence is achieved.

For the case of the spline ADI, however, in order to be able to evaluate the RHS in equations (11) and (12) with fourth-order accuracy (at convergence), it is necessary to obtain a fifth-order

interpolating polynomial approximating the new values of the stream function and of the vorticity along each row and column of the computational grid. This is done by solving two tridiagonal systems, formally identical to equation (6), for each row and for each column of grid points, which allow evaluation of the four matrices $K\psi\xi_{i,j}$, $K\psi\eta_{i,j}$, $K\omega\xi_{i,j}$ and $K\omega\eta_{i,j}$; from these, all the corresponding first and second derivatives, $m\psi\xi_{i,j}$, $M\psi\xi_{i,j}$, etc., can then be evaluated explicitly, by means of expressions formally identical to equations (4) and (5). As far as the boundary conditions are concerned, for the case of equation (6), the first and last values of K are evaluated by linear or quadratic extrapolations from the neighbouring points. It is noteworthy that in the present spline ADI technique, if an $N \times N$ mesh is used, at each ADI sweep it is necessary to solve $2N$ 2×2 block-tridiagonal systems (equations (7)–(10)) and $4N$ simple tridiagonal systems (equations of the type of equation (6)). A standard spline ADI would require the solution of $2N$ 4×4 block-tridiagonal systems, i.e. a lot more computational work. Also, the additional work of the present simplified spline ADI method with respect to the corresponding ADI approach is minimal, considering the accuracy improvement it provides.

The present approaches solve, at each sweep, the vorticity and the stream function equations as a coupled set on each row and column of the computational grid. For this reason it is possible, in the solution routine for each 2×2 block-tridiagonal system, to accommodate the double specification on the stream function at the boundary and to evaluate the vorticity at the wall, directly. For the case of the ADI method, the boundary conditions are imposed exactly as in Reference 1, with the difference that, in the present case, the incremental approach is used also at the first sweep of the ADI method. For the case of the spline ADI method, the boundary conditions have to be imposed in such a way that, at convergence, they are to be fourth-order accurate, consistently with the numerical scheme. Dirichlet boundary conditions are obvious, insofar as, if ω or ψ are prescribed at the boundary, it is required that

$$D\tilde{\psi} = D\tilde{\omega} = D\psi = D\omega = 0 \tag{17}$$

at the appropriate boundary grid points. A Neumann boundary condition for the stream function is slightly more complicated to deal with. Here only one example will be given, namely how to impose the boundary condition $\psi_\eta = 0$ at the lower wall boundary, in the first sweep of the spline ADI method. By omitting the i subscript, for convenience, we have

$$\frac{\tilde{\psi}_2 - \tilde{\psi}_0}{2h} + h(K\psi\eta_0 - K\psi\eta_2)/12 = 0 \tag{18}$$

Owing to the extra unknown $\tilde{\psi}_0$ (relative to a mirror image grid point), the steady-state stream function equation at the wall grid point is also employed, namely

$$\frac{\tilde{\psi}_2 - 2\tilde{\psi}_1 + \tilde{\psi}_0}{2h^2} + K\psi\eta_1/2 + \tilde{\omega}_1 = 0 \tag{19}$$

Equation (18) is then used to eliminate $\tilde{\psi}_0$ from equation (19), which, written in delta form, ($\tilde{\psi}_1 = 0$) becomes

$$\Delta\tilde{\omega}_1 + \Delta\tilde{\psi}_2/h^2 = -\omega_1^n - \psi_2^n/h^2 - \frac{K\psi\eta_0 + 6K\psi\eta_1 - K\psi\eta_2}{6} \tag{20}$$

Equation (20), coupled with the Dirichlet condition for the stream function ($\Delta\tilde{\psi}_1 = 0$) allows a direct evaluation of the incremental stream function and vorticity at the boundary. Obviously all the $K\psi\eta$ terms are known data at the old time level t^n and $K\psi\eta_0$ is evaluated from the neighbouring grid point values by linear or quadratic extrapolation. Several other boundary conditions are

possible; for example, using alternative expressions for m and M, which do not introduce a mirror-image grid point, or two different expressions for m, which amounts to enforcing that the spline interpolating polynomial has a continuous first derivative through the boundary grid point. In the present study all the approaches described above have been used successfully.

In Reference 1, an alternative, Crank–Nicolson-type, linearization and discretization in time of the governing equations was also used. The present techniques also have this option: in the computer programs all coefficients of the block-tridiagonal systems, to be solved at every sweep of the ADI methods, contain a CR coefficient which can be either 1 or 0·5, to provide the implicit backward (see, e.g., equations (9) and (10)) or the Crank–Nicolson time discretization, directly. The Crank–Nicolson approach is obviously second-order accurate in time, but, since the present techniques only provide the steady-state solution, this is not necessarily an advantage. Furthermore, when using a Crank–Nicolson averaging, in order to obtain a correct value of the vorticity at the wall, the boundary conditions have to be inconsistent with the difference equations; that is, it is necessary to use an implicit backward time discretization of the stream function equation at all boundary points in the $\sim$ sweep of the ADI methods, in order to obtain the correct vorticity at the wall at convergence. This result is consistent with what has already been observed by Hill *et al.*[9] and Briley and McDonald.[10] For this reason, most of the results later presented in this paper have been obtained with the fully implicit time discretization of equations (9) and (10). However, in some calculations, the Crank–Nicolson time linearization (which obviously produces identical results at convergence) has been found to provide faster convergence rates for the same values of the time step, k.

4. RESULTS

Flow between two rotating circles

The present methods have been developed in order to compute viscous steady flows past two-dimensional aerofoils, in connection with a method for generating a system of orthogonal curvilinear co-ordinates. The viscous flow between two concentric rotating circles has been considered as a model problem (somewhat simulating such a flow configuration), for which an exact solution is available for comparisons. The inner circle of radius equal to one is chosen to be stationary in order to test the no-slip, zero injection boundary conditions, usually given at the surface of a stationary aerofoil, whereas the outer circle rotates at such a speed that the vorticity on its boundary is also equal to one. A given vorticity has been imposed at the outer circle (of radius two), because, for external flow configurations, the outer boundary is usually chosen at a sufficient distance from the surface of the aerofoil, that a zero vorticity boundary condition is imposed. The physical flow field, divided into a system of equally spaced polar co-ordinates, has been transformed into a rectangle in the ξ, η plane. All metric coefficients and the Jacobian have then been evaluated numerically with fourth-order-accurate spline interpolating polynomials, except for the mixed derivatives which are identically zero. It is noteworthy that, owing to the co-ordinate transformation, the flow field is 'opened up', so that periodic boundary conditions are needed in the ξ direction. For more details and for an algorithm capable of solving periodic 2×2 block-tridiagonal systems, the reader is referred to Reference 1.

The results obtained with both the ADI and the spline ADI methods for such a test problem are given in Figure 1, where the stream function at the centre of the annulus and the vorticity at the wall of the inner circle are plotted versus the inverse of the number of meshes (h), squared (for the ADI method), and to the fourth power (for the spline ADI method), for several values of h. Two sets of spline ADI results are given, corresponding to the use of linear and quadratic extrapolations for the

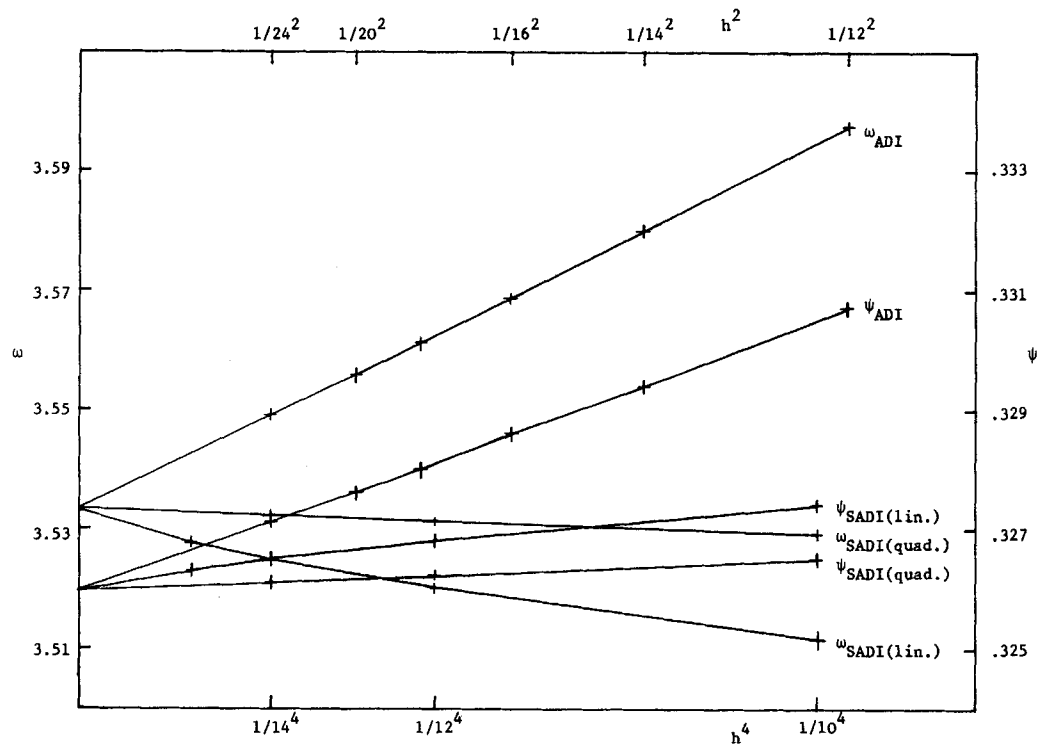

Figure 1. Numerical results for annulus flow

K spline functions. All results are seen to tend to the exact solution as h tends to zero and with the correct second-order-accuracy and fourth-order-accuracy, respectively. Also, the higher order extrapolation is seen to produce more accurate results, as expected. However, the most interesting point to make is that, whereas the computation costs are almost equivalent (the convergence rate is almost the same for both approaches, probably due to the one-dimensional nature of the problem), the more accurate spline ADI results, using a 10×10 mesh, have a discretization error up to five times smaller than that of the ADI results, using a 24×24 mesh.

The driven cavity flow

The classical driven cavity problem[11] was also used as a test problem to verify the present numerical techniques. The $Re = 100$ case has been considered, using a uniform rather coarse 14×14 mesh. The values of the vorticity at the centre of the moving wall of the cavity and the maximum value of the stream function are given in Table I for the ADI method as well as for the spline ADI method using either linear or quadratic extrapolation for the spline boundary conditions. A reference, accurate solution due to Rubin[11] is also provided for easy comparison. The ADI results are seen to be reasonably accurate and coincide with those obtained by Rubin,[11] using the same spatial discretization and mesh (15×15 grid points). The spline ADI results are considerably more accurate as far as the maximum value of the stream function is concerned. However, using a quadratic extrapolation for the spline coefficient $K\omega$ at the boundary is seen to produce a less accurate wall vorticity. This (apparently strange) result can be explained by considering that the vorticity and its second derivatives $K\omega$ vary very rapidly near the wall, so that

Table I. Driven cavity results

$Re = 100$	ω_{MTP}	ψ_{max}	
ADI	−8·916	−0·0874	
Spline ADI (linear extrap.)	−8·557	−0·0941	(14 × 14 mesh)
Spline ADI (quadr. extrap.)	−9·380	−0·0992	
Ref. solution[11]	−6·574	−0·1034	
$Re = 1000$			
ADI (20 × 20 mesh)	−17·292	−0·0913	
ADI (30 × 30 mesh)	−15·922	−0·1055	
Ref. solution[11]	−14·890	−0·117	

using a quadratic extrapolation for $K\omega$ on a coarse mesh may actually lead to a larger truncation error than a formally less accurate linear extrapolation. It is noteworthy that the results in Table I have been obtained using both the backward and Crank–Nicolson time discretization and values of A and B equal to or greater than 1. Also, all of the $Re = 100$ results have been obtained within 2 CPU minutes on an HP 1000/F minicomputer, thus verifying the efficiency of the proposed methods.

The rather difficult case $Re = 1000$ has also been considered using the ADI method and a uniform 20 × 20 mesh: although a converged solution has been obtained (an impossible task for the method of Reference 1) its accuracy is very poor insofar as the mesh employed is completely incapable of capturing the thin boundary layer near the walls of the cavity. Therefore, the following stretching has been employed which transforms a suitable non-uniform grid in the physical x, y plane into a uniform grid in the computational ξ, η plane:

$$\begin{pmatrix} x \\ y \end{pmatrix} = 0{\cdot}5 + 0{\cdot}5 \tanh\left[C \begin{pmatrix} 2\xi - 1 \\ 2\eta - 1 \end{pmatrix} \right] \Big/ \tanh(C) \tag{21}$$

It is noteworthy that by increasing the value of the arbitrary constant, C, more and more grid points are clustered near the walls of the cavity, whereas for a very small C a uniform grid is practically recovered. Here, numerical results have been obtained using both 20 × 20 and 30 × 30 meshes and always $C = 1{\cdot}8$. The results, given in Table I, are very reasonable (especially for the finer mesh) when compared to the reference solution of Rubin.[11] Without any attempt to optimize the time step, using a backward Euler time discretization, a full convergence (average residual 10^{-5}) required about 2000 or 3000 iterations ($k = 0{\cdot}03$ or $0{\cdot}02$) and 1 or 3 hours of CPU time, respectively.

Flow in a channel of complex geometry

The present methods were finally used to compute viscous laminar flow inside a channel of complex geometry. The problem was first proposed by Roache[12] who numerically verified that, if the length of the channel is scaled proportionally to the Reynolds number of the flow, self similar flow conditions are obtained for very high Re values. Recently the same problem has been used as a numerical test-case for comparing the accuracy and efficiency of several numerical Navier–Stokes solvers by the IAHR working group on refined modelling of flows at its VIth meeting held in Rome (24–25 June, 1982). The geometry of the channel is given in Figure 2(a) for the $Re = 10$ case and

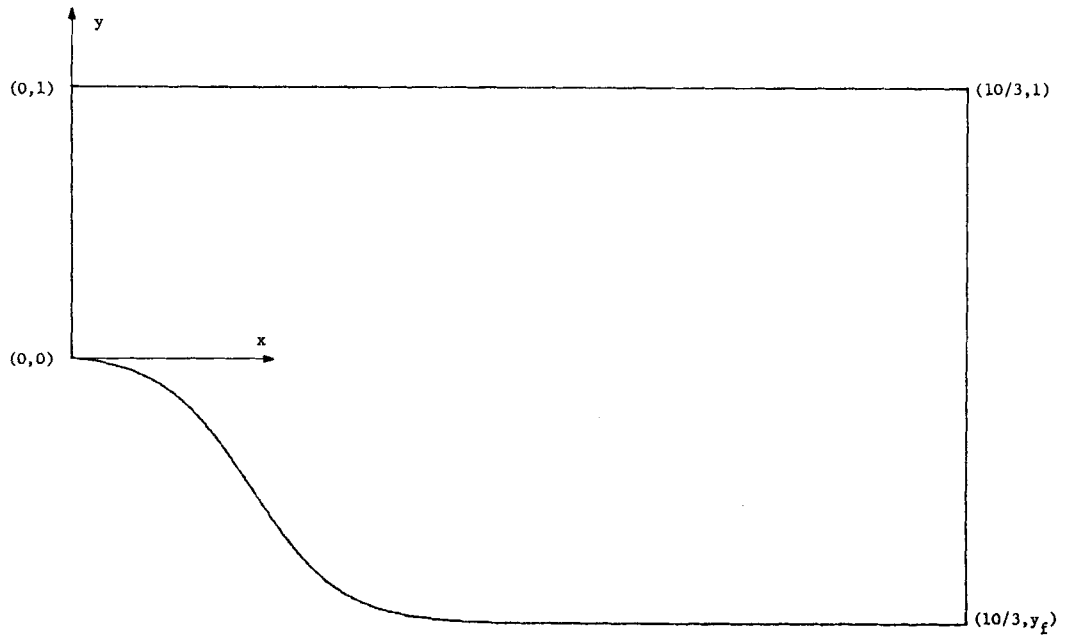

Figure 2(a). $Re = 10$ channel geometry

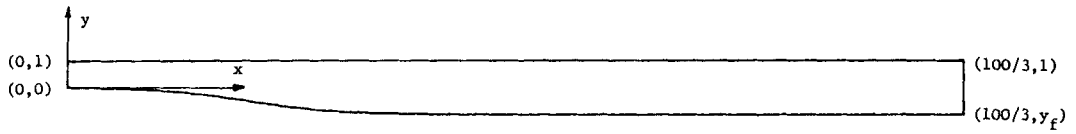

Figure 2(b). $Re = 100$ channel geometry

Figure 2(b) for the $Re = 100$ case. The lower wall of the channel is given analytically as

$$Y_l = \tfrac{1}{2}[\tanh(2 - 30x/Re) - \tanh 2] \tag{22}$$

and its centreline as

$$Y_u = 1 \tag{23}$$

The inlet and outlet sections of the channel are finally given as

$$x = 0 \quad \text{and} \quad x = Re/3 \tag{24a, b}$$

so that, with reference to Figures 2(a) and (b), $y_f = [\tanh(-8) - \tanh(2)]/2$

In the present study, a system of orthogonal, curvilinear coordinates has been used to map the physical (x, y) flow domain into a rectangle in the (ξ, η) computational domain. A simple algebraic transformation, as given by Blottner and Ellis[13] and described by Davis,[14] has been used for simplicity as well as for taking full advantage of the shape of the channel, being prescribed analytically. The system of (η = constant) co-ordinate lines in the physical plane has been prescribed as follows: the line $\eta = 0$ coincides with the lower boundary (the wall) of the channel and the line $\eta = 1$ with its upper boundary (the symmetry line). All the other $\eta = (j - 1)\Delta\eta (j = 2, 3, \ldots,$

$N+1, \Delta\eta = 1/N$) are given by the following expressions

$$Y_j = \frac{q^N - q^{j-1}}{q^N - 1} Y_l(x) + \frac{q^{j-1} - 1}{q^N - 1} Y_u(x) \tag{25}$$

A family of (ξ = constant) lines, orthogonal to the η = constant lines have then been obtained by integrating numerically with a fourth-order-accurate Runge–Kutta procedure, the following equation

$$\left(\frac{\partial x}{\partial \eta}\right)_\xi = -\frac{\left(\frac{\partial y}{\partial x}\right)_\eta \left(\frac{\partial y}{\partial \eta}\right)_x}{1 + \left(\frac{\partial y}{\partial x}\right)_\eta^2} \tag{26}$$

starting from prescribed points at the lower boundary of the channel. A few points are of interest: the distance between two successive η = constant lines in the physical plane has been chosen to increase at a constant rate ($q = 1{\cdot}1$) starting from the lower boundary. In this way a finer resolution is obtained near the wall of the channel where viscous effects are more important. The distance between two successive ξ = constant lines along the x co-ordinate in the physical plane has also been chosen to increase at a constant rate ($r = 1{\cdot}054$), starting from the point $x_i = Re/15$ (where the lower boundary of the channel has an inflexion point) in both $x > x_i$ and $x < x_i$ directions. In this way a finer resolution is obtained in the region where a separation bubble is likely to develop. Finally, the $\xi = 0$ and $\xi = 1$ lines in the physical plane have been chosen to coincide with the entrance and the exit of the channel, i.e. with the $x = 0$ and $x = Re/3$ lines, for convenience, and are not perfectly orthogonal to the η = constant lines. Therefore, the metric coefficients multiplying the mixed derivatives in the governing Navier–Stokes equations are not identically zero at all grid points and the accuracy of the spline ADI method slightly deteriorates locally, insofar as the mixed derivatives are evaluated with standard second-order-accurate central differences. The curvilinear co-ordinates, generated as described above, are shown in Figure 3 for the $Re = 10$ case, together

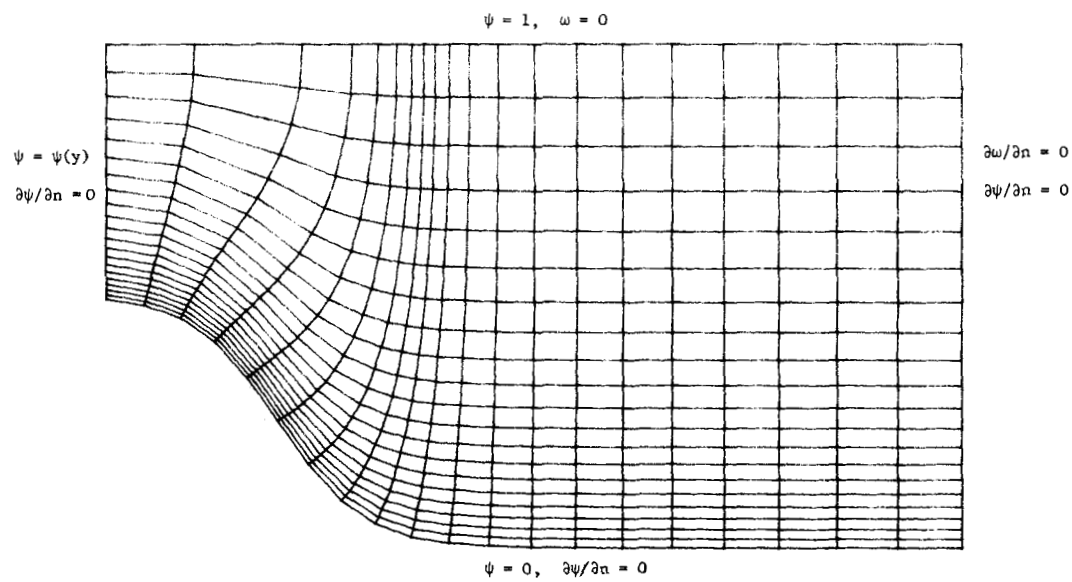

Figure 3. $Re = 10$ computational grid and boundary conditions

Table II. Channel flow ADI and spline ADI wall vorticity results

		SADI		ADI	
i	x	$Re = 10$	$Re = 100$	$Re = 10$	$Re = 100$
1	0·0	3·0756	3·0769	3·0113	2·9970
2	0·1477	2·5877	2·5393	2·6612	2·5620
3	0·2879	2·1025	1·9546	2·0040	1·9564
4	0·4209	0·9908	1·1806	0·9675	1·1820
5	0·5470	0·1826	0·4915	0·2148	0·4999
6	0·6666	−0·0864	0·0992	−0·0837	0·1075
7	0·7862	−0·1314	−0·0679	−0·1365	−0·0621
8	0·9123	−0·1145	−0·1227	−0·1184	−0·1189
9	1·0453	−0·1024	−0·1261	−0·1037	−0·1245
10	1·1855	−0·1025	−0·0930	−0·1032	−0·0901
11	1·3333	−0·0986	−0·0349	−0·0993	−0·0327
12	1·4891	−0·0752	0·0431	−0·0761	0·0482
13	1·6534	−0·0292	0·1281	−0·0307	0·1307
14	1·8266	0·0337	0·2158	0·0313	0·2212
15	2·0092	0·1056	0·2966	0·1024	0·2985
16	2·2018	0·1798	0·3747	0·1762	0·3790
17	2·4048	0·2511	0·4399	0·2473	0·4396
18	2·6188	0·3147	0·5020	0·3114	0·5058
19	2·8445	0·3661	0·5507	0·3636	0·5470
20	3·0824	0·4001	0·5945	0·3986	0·5997
21	3·3333	0·4115	0·6415	0·4336	0·6525

with the boundary conditions used in the present calculations. After evaluating all the grid-point locations in the physical x, y plane (corresponding to a uniform Cartesian grid in the computational ξ, η plane), the metric coefficients $\alpha, \beta, \gamma, \sigma, \tau$, and the Jacobian of the transformation are evaluated at all internal grid points by means of central differences or fourth-order-accurate spline approximations in the ADI and spline ADI methods, respectively. At the boundary points the metric coefficients necessary to evaluate ω from the stream function equation are obtained by linear or cubic extrapolation from the neighbouring gridpoints. The numerical solutions obtained for the $Re = 10$ and the $Re = 100$ cases by means of both present ADI methods are given in Table II as the values of the vorticity at the wall versus the x_i locations of the ξ co-ordinate lines (the x_i values corresponding to $Re = 100$ have to be multiplied by 10). For convenience, these results are also plotted in Figures 4 and 5 for the $Re = 10$ and $Re = 100$ cases, respectively; the results obtained by means of the spline ADI method, using a coarser 10×10 mesh, are also given. All solutions are seen to coincide, for all practical purposes, and favourably compare with those obtained by means of several other methods (see, e.g., Reference 15). The 20×20 mesh spline ADI solution is the most accurate and the other two solutions have comparable accuracy. For the two ADI calculations, the minimum value of the vorticity at the wall is plotted versus the normalized number of iterations, to provide an idea of the convergence properties of the technique. A full convergence (to machine accuracy) has been obtained within about 130 and 150 iterations ($k = 0{\cdot}075$ and $k = 0{\cdot}08$) for the $Re = 10$ and $Re = 100$ cases, corresponding to less than 5 CPU minutes on the HP 1000/F minicomputer. If one considers that a reasonable convergence is obtained in about 40 per cent of the total number of iterations (see Figures 4 and 5), the efficiency of the present ADI approach is self evident. The spline ADI converged within 5 to 10 more iterations than the standard ADI using the same number of grid points, because a stability limitation on k had to be satisfied for $A = B = 1$.

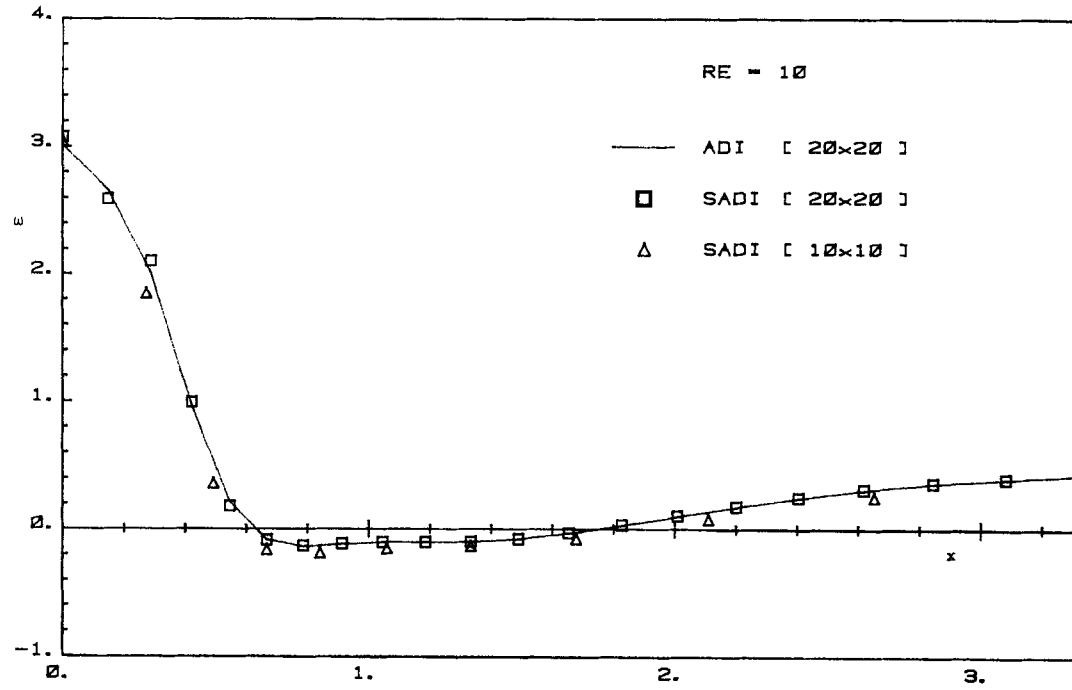

Figure 4. Wall vorticity

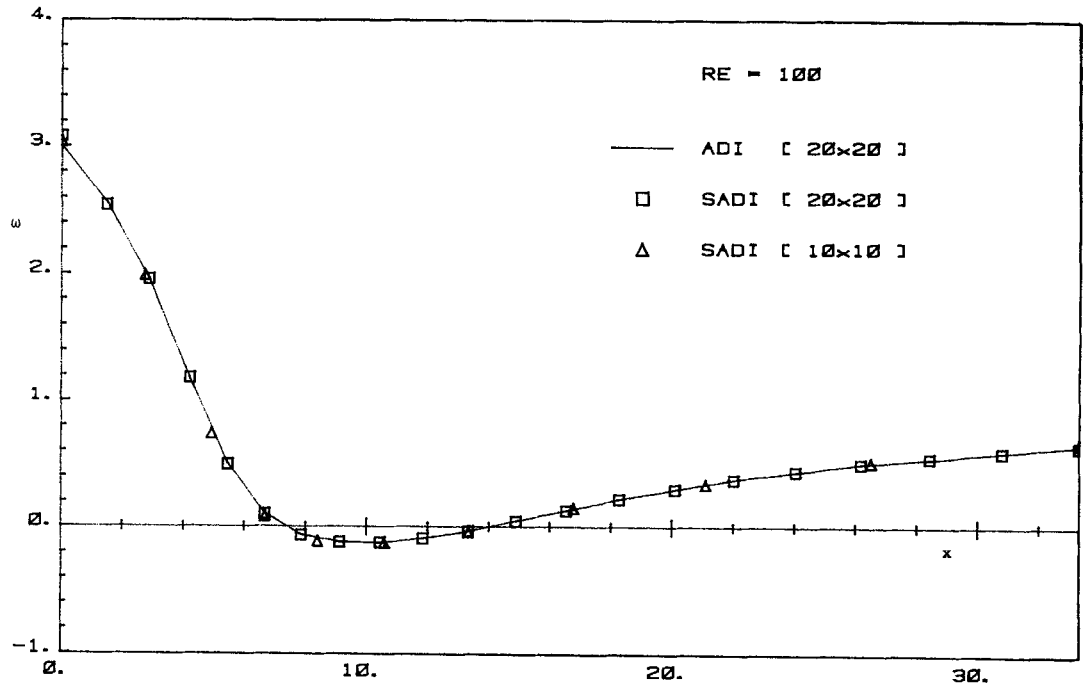

Figure 5. Wall vorticity

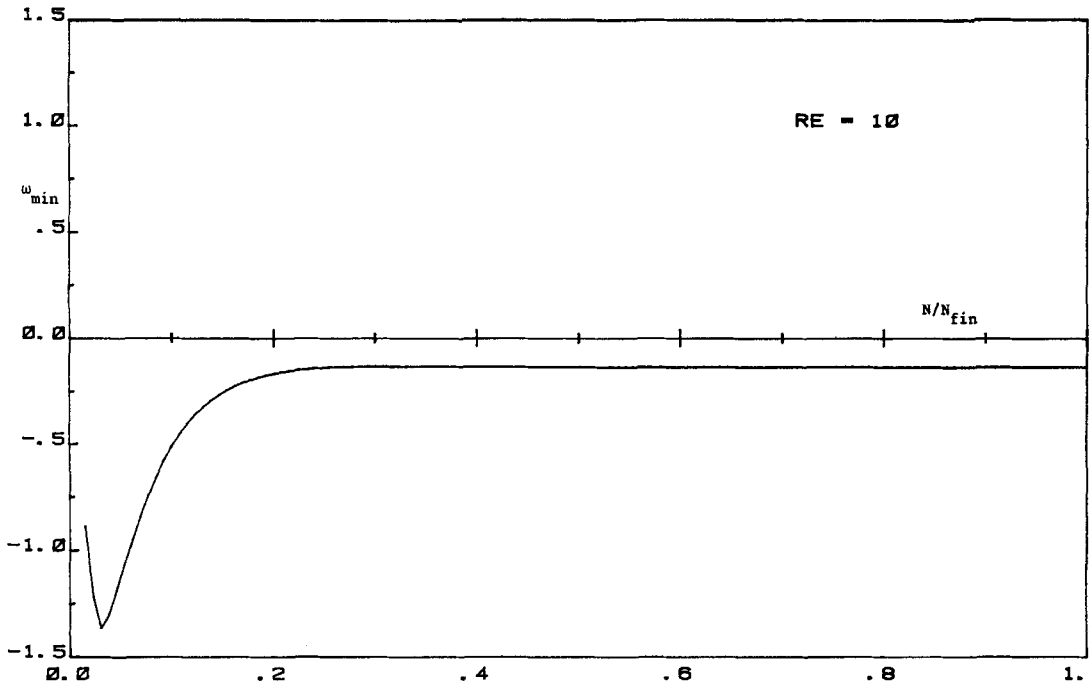

Figure 6. Minimum wall vorticity versus normalized iteration number

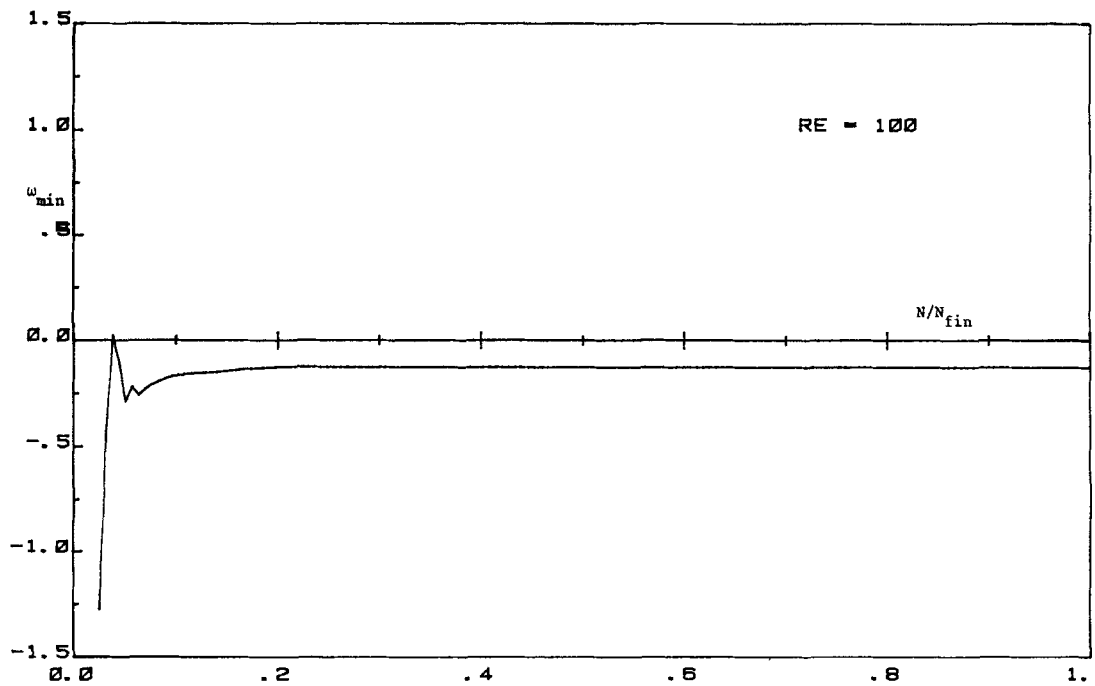

Figure 7. Minimum wall vorticity versus normalized iteration number

An optimization of the convergence, obtained by using different values of A and B, or by correcting the ADI solution only after a given number of ADI cycles, has not been pursued. However, by comparing the ADI solutions with the 10×10 mesh spline ADI solutions (which have comparable accuracy), it turns out that these required about 20 per cent less CPU time.

5. CONCLUSIONS

An improved ADI numerical technique for the solution of incompressible viscous steady flows has been developed, together with a fourth-order-accurate spline ADI method obtained by applying a spline deferred corrector approach to the present ADI technique. The validity and efficiency of the present approaches have been demonstrated by their application to the numerical solution of three viscous flow problems.

ACKNOWLEDGEMENTS

This research was performed in part at the AFWAL/FIMM, in summer 1981, under Project Number 2307N603, whose AFWAL task engineer was Dr. W. L. Hankey and was also supported by the Italian National Research Council (CNR). The calculations of the flow in a channel of complex geometry have been performed in co-operation with V. Magi, whose care and thoroughness were of invaluable help. The author is very grateful also to Dr. Hankey and Dr. Shang, for their interest and encouragement and to Prof. S. G. Rubin, for many precious discussions and helpful suggestions.

LIST OF SYMBOLS

A, B	Arbitrary constants in the spline deferred corrector approach
C	Arbitrary constant in the stretching equation (21)
c	Constant in Burgers' equation
D	Incremental operator, applied to any variable
h	Step size in the space variable
J	Jacobian of the co-ordinate transformation
k	Time step
K	Spline coefficient, related to its second derivative
m	Spline first derivative
M	Spline second derivative
t	Non-dimensional time
x	Non-dimensional horizontal co-ordinate
y	Non-dimensional vertical co-ordinate
u	Dependent variable in Burgers' equation
Y_l, Y_u	Lower and upper boundaries of the channel
$\alpha, \beta, \gamma, \sigma, \tau$	Scale factors of the co-ordinate transformation
η	Vertical transformed co-ordinate
ν	(Non-dimensional) kinematic viscosity in Burgers' equation
ξ	Longitudinal transformed co-ordinate
ψ	Stream function
ω	Vorticity

Subscripts

$i, i+1, i-1$	Longitudinal grid points
$j, j+1, j-1$	Vertical grid points
t, x, y, ξ, η	Partial derivative with respect to the indicated variable

Superscripts

$n, \sim, n+1$	(Time) levels of the ADI techniques

REFERENCES

1. M. Napolitano, 'Simulation of viscous steady flows past arbitrary two-dimensional bodies', in *Numerical Methods for Nonlinear Problems*, Pineridge Press, 1980, pp. 721–733. Also AFWAL-TR-80-3038.
2. J. Douglas and J. E. Gunn, 'A general formulation of alternating direction methods', *Numerische Mathematik*, **6**, 428–464 (1964).
3. P. K. Khosla and S. G. Rubin, 'A diagonally dominant second-order-accurate implicit scheme', *Computers and Fluids*, **2**, 207–209 (1974).
4. R. M. Beam and R. F. Warming, 'An implicit factored scheme for the compressible Navier–Stokes equations', *AIAA J.*, **16**, (4), 393–402 (1978).
5. S. G. Rubin and P. K. Khosla, 'A simplified spline solution procedure', Presented at the 6th ICNMFD, Tblisi, URSS, 1978, in *Lecture Notes in Physics*, no. 90, pp. 468–476, Springer Verlag.
6. S. G. Rubin and P. K. Khosla, 'Polynomial interpolation methods for viscous flow calculations', *J. Comp. Phys.*, **24**, 217–244 (1977).
7. F. C. Thames, J. F. Thompson, C. W. Mastin and R. L. Walker, 'Numerical solutions for viscous and potential flow about arbitrary two-dimensional bodies using body-fitted coordinate systems', *J. Comp. Phys.* **24**, 245–273 (1977).
8. R. T. Davis, 'Numerical solution of the Navier–Stokes equations for symmetric laminar incompressible flow past a parabola', *J. Fluid Mech.*, **51**, (3), 417433 (1972).
9. J. A. Hill, R. T. Davis and G. L. Slater, 'Development of a factored ADI scheme for solving the Navier–Stokes equations in stream function vorticity variables', *AFL Report No. 79–12–48*, Dept. of Aerospace Engineering and Applied Mechanics, University of Cincinnati, December 1979.
10. W. R. Briley and H. McDonald, 'Solution of the multidimensional compressible Navier–Stokes equations by a generalized implicit method', *J. Comp. Phys.* **24**, 372–397 (1977).
11. S. G. Rubin, 'Incompressible Navier–Stokes and parabolized Navier–Stokes solution procedures and computational techniques', *VKI Lecture Series 1982–5*, Rhode St. Genese, Belgium, 29 *March*–2 April 1982.
12. P. J. Roache, 'Scaling of high Reynolds number weakly separated channel flows', *Symposium on Numerical and Physical Aspects of Aerodynamic Flows*, California State University, Long Beach, Ca 19–21 January 1981.
13. P. R. Blottner and M. A. Ellis, 'Finite difference solution of the incompressible three-dimensional boundary layer equations for a blunt body', *Computers and Fluids*, **1**, 133–158 (1973).
14. R. T. Davis, 'Notes on coordinate generation', *VKI Lecture Series 1981–5*, Rhode St., Genese, Belgium, 30 March–3 April 1981.
15. L. Quartapelle and M. Napolitano, 'Finite element solution to the time-dependent vorticity–stream function equations in split form', *International Symposium on Refined Modelling of Flows*, Paris, 7–10 September 1982.